Conclusion

The changes in the relative intensities of the Raman lines in the C–H stretching region in going from the crystal to liquid crystal to isotropic phases are indicative of pseudocrystalline intermolecular interactions in the liquid-crystalline phase. Regions of local order, relatively unperturbed during the time of a vibration, exist in the liquid crystal even when no external fields are aligning the mesophase. It is interesting to note that the hydrocarbon side chain, with the possible exception of the methyl group, does not reflect the changes in local symmetry at the phase transitions. Although this side chain is purported to play a major role in the structure of cholesteric phases, it may be in a "liquid" state even in the liquid-crystalline phase.

The results for mixed cholesteric liquid crystals support the idea that the phases are completely homogeneous, with intermolecular forces different from those in either pure component.

Further work on these and other systems is in progress.

Acknowledgments. This work was supported by a grant from the U. S. Army Research Office–Durham. We are grateful to Hoffmann-La Roche, Inc. for samples of ethylestrenol and 19-nortestosterone.

Electron Paramagnetic Resonance Studies of Ketyl Ion Pairs in Ethereal and Polar Solvents[1]

K. S. Chen, S. W. Mao, K. Nakamura, and N. Hirota*

Contribution from the Department of Chemistry, State University of New York at Stony Brook, Stony Brook, New York 11790. *Received December 30, 1970*

Abstract: Detailed studies on the structures of ion pairs of ketyls in ethereal solvents (THF and DME) and mixtures of DME and DMF are reported. Temperature dependence of the alkali metal splittings in ethereal solvents and its connection to the ion pair structure are considered in detail. The effects of the addition of DMF on the structures of ion pairs were investigated. The addition of small amounts of DMF produces DMF-solvated ion pairs. Detailed thermodynamic and kinetic studies of the solvent-exchange processes have been made in DME–DMF mixtures. The lifetimes of DMF-solvated species are determined at low temperatures. In solutions containing large fractions of DMF, dissociation–association equilibria take place. Estimates of equilibrium constants and association and dissociation rate constants were made from epr spectra. It is shown that ketyls never exist as solvent-separated ion pairs under the conditions employed here. The factors which determine the ion pair structures are discussed.

The structural and kinetic properties of ion pairs of radical ions and carbanions have been the subjects of current interest, and a number of detailed investigations have been made in recent years.[2] From spectroscopic[2–4] (epr, nmr, visible, uv) and conductometric studies,[5] some detailed models of ion pair structures were proposed. Ion paris of hydrocarbon radical ions[3b,c,5] and carbanions[3a] in ethereal solvents have been investigated most thoroughly so far. It now seems to be well established that different structures of ion pairs, such as contact (tight) and solvent-separated (loose) ion pairs,[6] exist in many hydrocarbon anion systems. On the other hand, ion pairs made of other than aromatic hydrocarbons are much less studied and there still remain a number of questions to be answered concerning the properties of ion pairs. For example, it is not well known whether or not the same model of ion pair can be applied generally to many different types of systems, including the ion pairs made of radical anions with more localized charge densities such as ketyls. The cause of temperature dependence of alkali metal splittings in the epr spectra of radical ions such as ketyls is not well understood. The factors which determine the structures of ion pairs are not completely understood.

In radical ions, such as ketyls, the negative charges are more localized on the carbonyl groups. Thus the electrostatic interaction between positive and negative ions is expected to be much stronger than in hydrocarbon ion pairs. Therefore, contact ion pair structures are expected to prevail in such ion pairs. In fact, epr data indicate contact ion pair structures for ketyls in ethereal solutions.[7] Then the following questions may arise. (1) What is the cause of the large temperature dependence of alkali metal splittings in such systems, if the ion pairs are contact pairs and there exist no dynamic equilibria between contact and solvent-separated pairs? Is the process producing the

(1) This work was supported by a grant from the National Science Foundation and a research fellowship from the A. P. Sloan Foundation to N. H.

(2) (a) M. Szwarc, *Accounts Chem. Res.*, 2, 187 (1969); (b) M. C. R. Symons, *J. Phys. Chem.*, 71, 172 (1967).

(3) (a) T. E. Hogen-Esch and J. Smid, *J. Amer. Chem. Soc.*, 88, 107, 319 (1966); (b) N. Hirota and R. Kreilick, *ibid.*, 88, 614 (1966); (c) N. Hirota, *J. Phys. Chem.*, 71, 127 (1967); *J. Amer. Chem. Soc.*, 90, 3603, 3611 (1968).

(4) L. L. Chan and J. Smid, *ibid.*, 89, 4547 (1967).

(5) (a) C. Carvajal, J. K. Toelle, J. Smid, and M. Szwarc, *ibid.*, 87, 5548 (1965); (b) R. V. Slates and M. Szwarc, *J. Phys. Chem.*, 69, 4124 (1965); (c) P. Chang, R. V. Slates, and M. Szwarc, *ibid.*, 70, 3180 (1966).

(6) The term "contact ion pair" may not be very accurate here, since the separation between positive and negative ions is larger than expected from the ionic radii of the two ions because of solvation. Contact ion pair is used to represent tight ion pairs in which no solvent is present between the two ions.

(7) T. Takeshita and N. Hirota, *J. Amer. Chem. Soc.*, in press.

temperature dependence still a dynamic equilibrium between structurally different ion pairs or is it a static change of the structures of the ion pairs?[8] (2) Can tightly bound ion pairs, such as ketyls, exist as solvent-separated ion pairs in more polar solvents? How does the nature of the solvent affect the structures of ion pairs? How does the nature of anions affect the structures of ion pairs?

In this paper we tried to answer these questions and discuss three major topics. First, the temperature dependence of alkali metal splittings was studied over very wide ranges of temperature and discussed in terms of a dynamic model. New observations which seem to support the dynamic model are presented and the rate constants associated with the dynamic process are estimated. Second, we have studied the effect of the addition of a polar solvent, DMF, on the structures of ion pairs. We have found that ketyls never exist as solvent-separated ion pairs even in mixtures of DME and DMF, but DMF preferably solvates cations, forming DMF solvated ion pairs. This result is strikingly different from the results of previous studies on the effect of polar solvents on the structures of ion pairs in other systems.[3a,9] Since DMF-solvated ion pairs have different alkali metal splittings, one can investigate the details of the thermodynamics and kinetics of the solvent exchange processes. These are described in detail. Finally, in solutions containing large fractions of DMF, ketyls dissociate into free ions. Equilibrium and kinetic studies on association and dissociation processes were made and the lifetimes of the free and associated species were estimated under various conditions.

Experimental Section

Radical ions in ethereal solvents (DME and THF) were prepared according to standard procedures already described elsewhere.[10] Samples in mixtures of DMF and ethereal solvents were made by first preparing radical ions in ethereal solvents and then introducing the desired amount of purified DMF through a high-vacuum line. DMF was stored in an evacuated container with fluorenone or benzophenone ketyls in order to ensure the absence of air, moisture, or any other radical scavengers in the solvents. In order to cut the time required to transfer DMF, it was necessary to use a very short transfer line.

All of the epr measurements were made with a Varian V-4502 spectrometer according to the procedures described in a previous paper.[10] In order to take the spectra at temperatures from 60 to 160°, solutions containing desired amounts of radical ions were sealed into glass tubings of 4-mm o.d. and approximately 8 cm long. All of the visible spectra were taken wth a Cary-14 spectrophotometer using a 1-cm path length cell. The approximate determinations of concentrations were made for some fluorenone samples from visible spectra. A standard sample for concentration determination was made by reducing a known amount of fluorenone to mononegative ion as much as possible, but avoiding conversion of it to dinegative ions.

The measurements of line broadening for kinetic studies were made from intensity measurements, in most cases, assuming that the intensities are inversely proportional to the squares of line widths. In some systems overlapping of nearby lines causes uncertainties in intensity measurements. In those cases, estimates were made by comparing the observed line shapes with those calculated for known splittings and line widths.

(8) Static structural changes of ion pairs have been suggested for some ion pair systems: G. W. Canters, E. deBoer, B. M. P. Hendriks, and A. A. K. Klassen, *Proc. Colloq. AMPERE, 1968*, **15**, 242 (1969).
(9) C. Y. Lin and J. Gendell, *J. Chem. Phys.*, **47**, 3475 (1967).
(10) N. Hirota, *J. Amer. Chem. Soc.*, **89**, 32 (1967).

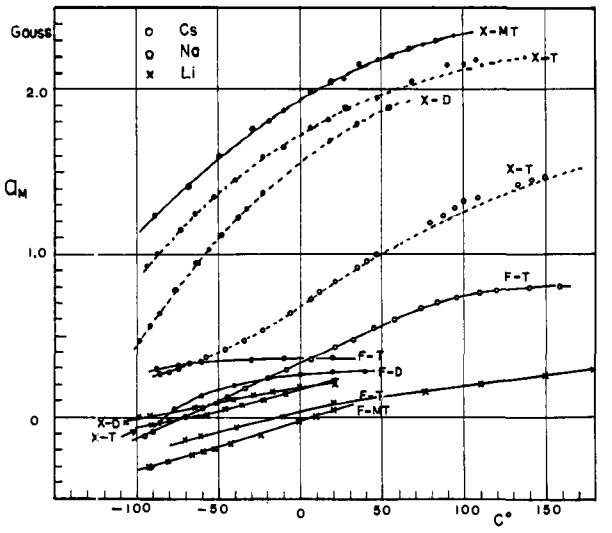

Figure 1. Temperature dependence of alkali metal splittings: Cs, ●; Na, O; and Li, ×. X and F stand for xanthone and fluorenone, respectively; T, MT, and D represent THF, MTHF, and DME. Dotted lines give the predicted temperature dependence curves calculated by using the two-jump models with the constants a_A = 0.1 G and a_B = 2.7 G for cesium xanthone in THF, a_A = −0.1 G and a_B = 2.6 G for cesium xanthone in DME, and a_A = 0.2 G and a_B = 2.2 G for sodium xanthone in THF. The other lines were drawn to fit the experimental values smoothly.

Results and Discussion

Structures of Ion Pairs in Pure Ethereal Solvents. As reported previously, alkali metal splittings of ketyls show very marked temperature dependence.[11,12] More complete data concerned with the temperature dependence of alkali metal splittings in various fluorenone and xanthone ketyls over very wide ranges of temperature are summarized in Figure 1.

Some characteristic features of the temperature dependence of alkali metal splittings of ketyls are summarized in the following. (1) In most systems, the temperature dependence is very large. In several systems, such as cesium fluorenone and sodium fluorenone in THF, the alkali metal splittings seem to approach limiting values at high temperatures. (2) Alkali metal splittings are solvent dependent for most cations. Even cesium splittings show strong solvent dependence. (3) In general, splittings for xanthone systems are much larger than those for fluorenone systems, although the general trend of the temperature dependence is similar. All the splittings in fluorenone appear to change sign and become negative at very low temperature, whereas all the splittings except lithium splittings in xanthone remain positive even at the lowest temperature used. (4) Cesium splittings are generally quite temperature and solvent dependent. This is different from the cases of hydrocarbon anions, where cesium splittings are relatively insensitive to temperature and solvent.[3b,c]

These observations indicate the importance of the solvation process in determining the structures of ion pairs in all ketyls, as in hydrocarbon anion cases. Even with large cations such as cesium, solvation of

(11) N. Hirota, "Radical Ions," E. T. Kaiser and L. Kivan, Ed., Wiley, New York, N. Y., 1968, Chapter 2.
(12) N. Hirota and S. I. Weissman, *J. Amer. Chem. Soc.*, **86**, 2536 (1964).

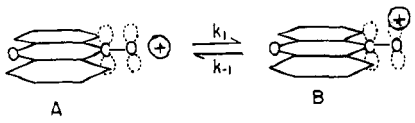

Figure 2. Dynamic model of structure changes of ion pairs.

the cation cannot be neglected in considering ion pair structures.

The general shapes of the temperature dependence curves are very similar to those found for hydrocarbon radical ions undergoing rapid ion pair equilibrium,[3b,c] although changes are much more gradual in ketyls. The temperature dependence of alkali metal splittings of many ion pairs of hydrocarbon radical ions, particularly those with sodium and lithium ions, were successfully interpreted by using two-jump processes between tight (contact) and loose (solvent separated) ion pairs.[3b,c] However, a similar interpretation cannot be applied here, because the structure is considered to be a contact ion pair at all temperatures.[7]

Since alkali metal splittings are extremely temperature dependent, the average positions of the metal ions with respect to anions must be changing with temperature in most ketyl systems. The alkali metal splittings (a_m) are then given by the time average over the different values in possible states i.[13]

$$a_m = \frac{\sum_i a_m^i \exp\left(-\frac{E_i}{RT}\right)}{\sum_i \exp\left(-\frac{E_i}{RT}\right)} \qquad (1)$$

Here a_m^i is the splitting in the ith state. The different states include all the states with different cation and anion configurations, including different vibrational states associated with each configuration. In ketyls the cation is assumed to be located in the neighborhood of oxygen. The MO calculation based on this assumption correctly predicts the trends of the change of g factors and ^{13}C and proton splittings upon ion pair formation.[7]

At very low temperatures the alkali metal splittings of many ketyls are generally very small, and in several cases they become negative. This fact seems to be best explained by assuming that the positive ions approach a position in the plane of aromatic molecule, namely, in the nodal plane of the $2p\pi$ oxygen orbital, at very low temperature (Figure 2). Although the exact mechanism of producing alkali metal splittings is not completely established yet, one may expect negative spin density at the alkali metal nucleus in this structure through indirect spin polarization.[14] At higher temperatures the splittings increase to quite large values. This is interpreted as arising from the change of the average position of the cation from a nodal-plane position to an off-nodal-plane position, as schematically shown in Figure 2. In a structure such as shown in Figure 2B, direct transfer of unpaired spin could give relatively large positive spin densities.[13,15,16] In view of the numerous observations[3] which suggest the occurrence of more solvation at lower temperature in most hydrocarbon ion pair systems, the preference for the structure shown in Figure 2A at low temperature seems to be reasonable, because more space for solvation is available for structure A.[17]

This view of the change in the position of the cation also seems to be consistent with observations of the effect of alcohol solvation of the ion pair structures reported in a preliminary note.[18] The alcohol solvates the oxygen atom by hydrogen bonding, as indicated by a large increase in ^{13}C splitting after the addition of a small amount of isopropyl alcohol. The solvation by an alcohol with a bulky alkyl group, such as isopropyl alcohol, increases the alkali metal splittings greatly. The increases of alkali metal splittings in THF at 25° are from 0.07 to 0.35 G for lithium, from 0.43 to 0.70 G for sodium, from 0.076 to 0.10 G for potassium, and from 0.34 to 0.38 G for cesium. The values obtained by alcohol addition are rather close to the high-temperature-limiting values in pure ethereal solutions. If the alcohol tends to block the nodal-plane position (A), the metal ion is pushed toward the off-nodal-plane position (B), and the ion pair will have larger splittings. However, there remains the question of the mechanism of making such changes. As in hydrocarbon anion cases, one can consider two limiting models.

(1) Static Model.[8] The position of the potential minimum for a positive ion moves gradually from A to B with temperature. The positive ion vibrates around the potential minimum.

(2) Dynamic Model.[3b,c] The existence of two or more potential minima is assumed. The cation jumps from one position of the potential minimum to the other, with varying probabilities of occupation at different positions with temperaure. The splitting at each position may change with temperature, but the major cause of the temperature dependence is considered to be the change in relative populations at different positions.

These two models are, of course, limiting, and models of a more intermediate nature may be realistic. For example, even if the dynamic model is applicable, the position of the potential minimum may change considerably with temperature. It is also rather meaningless to distinguish two models, if the conversion rates from one position to another become very fast so that the process can be considered almost as a cation vibration process. Nevertheless, such a distinction was found to be useful for hydrocarbon anions.

(13) N. M. Atherton and S. I. Weissman, *J. Amer. Chem. Soc.*, **83**, 1330 (1961).

(14) Although there is no direct experimental evidence for negative alkali metal splittings for the ion pair structure A of ketyls, recent nmr studies confirm that the alkali metal splittings for lithium and sodium 2,2′-dipyridyl are in fact negative. In these pairs cations are located in the nodal plane of the $2p\pi$ orbital as in the suggested ketyl structure A: T. Takeshita and N. Hirota, *Chem. Phys. Lett.*, **4**, 369 (1969).

(15) S. Aono and K. Ohashi, *Progr. Theor. Phys.*, **30**, 162 (1963).

(16) I. Goldberg and J. Bolton, *J. Phys. Chem.*, **74**, 1965 (1970).

(17) A potential energy calculation made by McClelland indicates that the most stable position for a cation in ketyl is on the carbonyl group, somewhere between the oxygen and carbon atoms [B. J. McClelland, *Trans. Faraday Soc.*, **57**, 1458 (1961)]. Gill and Warhurst also suggested similar structures for ketyls based on a comparison between optical and epr spectra [E. Warhurst and P. S. Gill, *ibid.*, **64**, 293 (1968)]. We think that neither of these arguments is applicable to ketyls in solution for the following reasoning. First, the calculation which does not take into account the solvation effect may not be applicable to the actual system in solution. Second, we think that the major species responsible for the optical absorption in the Gill–Warhurst experiments are ion aggregates, not ion pairs. Arguments based on such comparisons could be erroneous.

(18) K. Nakamura and N. Hirota, *Chem. Phys. Lett.*, **3**, 137 (1969).

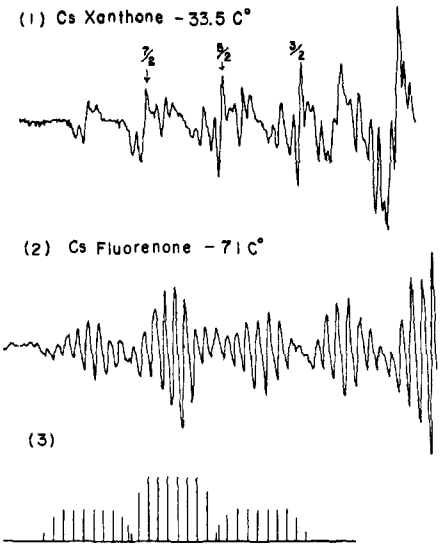

Figure 3. Initial part of the epr spectra of cesium xanthone and fluorenone at low temperature; the examples of M_z-dependent line width: (1) cesium xanthone in DME at −33.5°, $^7/_2$, $^5/_2$, and $^3/_2$ indicate the corresponding M_z of each peak; (2) cesium fluorenone in DME at −71°; (3) stick diagrams of the initial part of the epr spectra of cesium fluorenone in DME in the absence of M_z-dependent broadening at −71°.

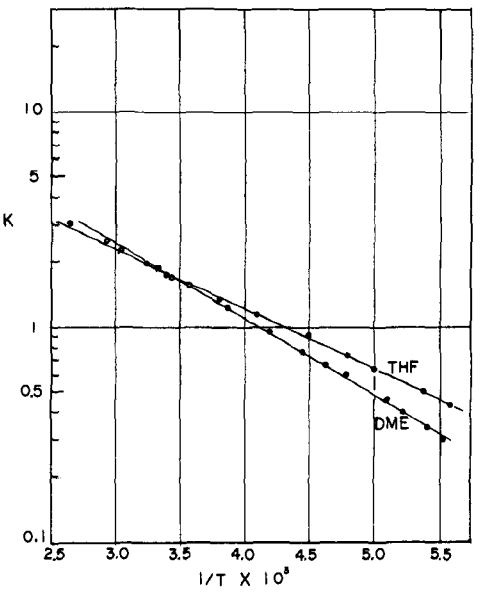

Figure 4. Plot of log K *vs.* $1/T$ for structure change of an ion pair. K values were calculated using the two-jump model with the following choice of a_A and a_B: cesium xanthone in THF, a_A = 0.1 G and a_B = 2.7 G; cesium xanthone in DME, a_A = −0.1 G and a_B = 2.6 G.

If the dynamic model is applicable and the rates involved in the dynamic processes are sufficiently slow, one should observe M_z-dependent line widths as observed in many hydrocarbon anion pairs undergoing rapid ion pair equilibrium.[3b,c] Therefore, we have carefully investigated the line widths of alkali metal splittings at low temperatures. Over the entire range of temperature, sodium ketyls in ethereal solution show no clear M_z-dependent line broadening, whereas all cesium ketyls studied here show clear M_z-dependent line broadening, as shown in Figure 3. Therefore, we think that the dynamic model is applicable at least in cesium ketyls.[19] We made an analysis based on this assumption. Accurate analysis of the M_z dependence of the line width is difficult because of the overlapping of lines, but M_z-dependent line broadening seems to be approximately proportional to M_z^2.

The shapes of the temperature-dependence curves of the alkali metal splittings of many ketyls are in fact very similar to those found in hydrocarbon anion cases undergoing ion pair equilibria. Therefore, it is tempting to apply the two-jump model to analyze the temperature-dependence curves. The metal splitting is given by[3b,c]

$$A \underset{k_{-1}}{\overset{k}{\rightleftharpoons}} B$$

$$a = \frac{a_A(T) + Ka_B(T)}{i + K} \qquad K = \frac{a_B(T) - a}{a - a_A(T)} = \frac{k_1}{k_{-1}} \quad (2)$$

$a_A(T)$ and $a_B(T)$ are the splittings in structures A and B at temperature T. In general, these splittings are considered to be temperature dependent. For many hydrocarbon ion pair systems, the simple model using constants a_A and a_B were very successful in explaining the observed temperature dependence. However, this assumption is probably not applicable in our systems, because the temperature ranges involved are very large. It is well known that the splittings in tight ion pairs in hydrocarbons are often temperature dependent, and a_A and a_B may be expected to be temperature dependent [3b,c] We have tried to fit the temperature-dependence curves using a simple two-jump model with constants a_A and a_B. With appropriate choices of a_A and a_B, it is possible to obtain very close agreement between the observed values and predicated ones in the cesium xanthone case, as shown in Figure 1 (dotted lines). Log K *vs.* $1/T$ plots using the constants a_A and a_B give very good straight lines over very large temperature ranges, as shown in Figure 4, although the choice of a_A and a_B is somewhat arbitrary. However, a complete fit cannot be made for sodium xanthone and fluorenone no matter how a_A and a_B were chosen. More satisfactory fits may be obtained by using the two-jump model if small temperature dependences of a_A and a_B are included.

If the two-jump model is applicable, the line width of the peak (ΔH_{M_z}) associated with the alkali metal magnetic quantum number M_z is given by

$$\Delta H_{M_z} = \alpha_{M_z} + \frac{P_A^2 P_B^2 (1 + K) M_z^2 (a_A - a_B)^2}{k_1} \quad (3)$$

(19) The M_z^2-dependent line broadenings in cesium splittings were previously found in cesium naphthalenide in DME and ascribed to some dynamic ion pair processes.[3b] Recently, W. G. Williams, R. J. Pritchett, and G. K. Fraenkel, *J. Chem. Phys.*, 52, 5584 (1970), suggested that the M_z^2-dependent broadening in this system may be due to incomplete averaging of the anisotropic part of hyperfine interaction. We would like to point out the following difficulty in this interpretation. Contrary to the case of a DME solution, cesium naphthalenide in THF and MTHF does not show M_z-dependent line broadening down to −90° (in the mixture of MTHF and DEE all cesium lines are sharp and have approximately same intensities even at −110°). If the M_z-dependent line broadening is due to incomplete averaging of anisotropic interaction, the rotational correlation times for these ion pairs must differ by more than an order of magnitude between DME and the other ethereal solvents. Since the viscosities of these solvents at low temperatures are not much different from each other, it seems more reasonable to assume that the rotational correlation times are similar. It is difficult to expect that the incomplete averaging of anisotropic part is so much different between DME and other ethereal solutions. Therefore, we think the M_z^2-dependent broadenings in cesium ion pairs are mainly due to cation motion in ion pairs, and modulation of isotropic splitting is the major source of broadening.

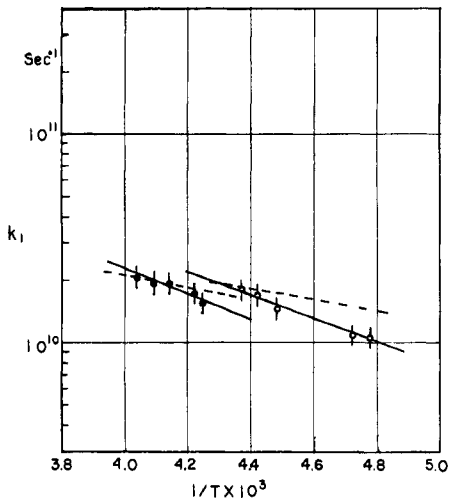

Figure 5. Plot of log k_1 *vs.* $1/T$ for the conversion rate of an ion pair structure. k_1 is estimated by using the two-jump model. Dotted lines indicate the estimated rates for k_{-1}: cesium xanthone in THF, ●; cesium xanthone in DME, ○.

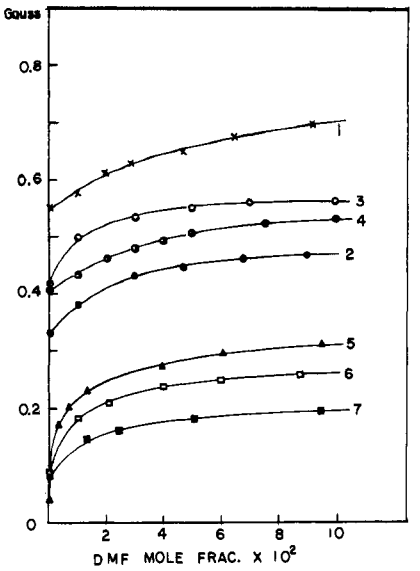

Figure 6. Change of metal splittings by the addition of DMF: (1) sodium xanthone, DME, −20°; (2) sodium xanthone, DME, −70°; (3) sodium fluorenone, THF, 23°; (4) sodium fluorenone, DME, 23°; (5) lithium fluorenone, MTHF, 23°; (6) lithium fluorenone, THF, 23°; (7) lithium fluorenone, DME, 23°.

Here P_A and P_B are the fractions of A and B structures. Strictly speaking, α_{M_z} depends on M_z, but this dependence may be neglected in our case compared to the M_z dependence of the second term. Then

$$k_1 = (2.03 \times 10^7)\frac{P_A^2P_B^2(1 + K)M_z^2(a_A - a_B)^2}{\delta H_{M_z}}$$

$$= (2.03 \times 10^7)\frac{K^2(a_A - a_B)^2(M_z^2 - M_z^2)}{(1 + K)^3(\delta H_{M_z} - \delta H_{M_{z'}})} \text{ sec}^{-1}$$

$$= (2.03 \times 10^7)\frac{K^2(a_A - a_B)^2(M_z^2 - M_{z'}^2)}{(1 + K)^3[(I_{M_{z'}}/I_{M_z})^{1/2} - 1]\Delta H_{M_{z'}}} \text{ sec}^{-1} \quad (4)$$

Here δH_{M_z} is the line broadening due to the motional process and I_{M_z} indicates the intensity of the M_z peak. Using the above formula, we have estimated k_1 and k_{-1} for cesium xanthone at various temperatures. M_z and $M_{z'}$ are $^7/_2$ or $^5/_2$ and $^3/_2$. The rate constants determined in this way are given in Figure 5. Because of the overlapping of the line widths and the uncertainties involved in estimating K and a_A and a_B, the numerical values estimated may have uncertainties up to 50%. Nevertheless, the analysis indicates that the cation jumping rate is $\sim 10^{10}$ sec^{-1} if the dynamic model is applicable. The precision of our measurement is not good enough to make an accurate estimate of activation energy, but E_a is estimated to be ~2.5 kcal of the k_1 process.

For cesium fluorenone, such calculations are difficult because of overlapping of lines. However, it is very clear that M_z-dependent broadening is taking place. The comparison between the stick diagram and the observed spectrum at low temperatures is given in Figure 3.

The absence of the M_z-dependent line broadening in sodium ketyls means either that the dynamic process does not exist or that the process is too fast to show the line width effect. The lower limit of the detectability of the line width variation under the present experimental conditions is about 3 mG. Therefore, for sodium xanthone at −60° using $\delta H_{3/2} - \delta H_{1/2} < 3 \times 10^{-3}$ G and $a_A - a_B \simeq 2$ G, we obtain a lower limit for k_1 of $\sim 10^9$ sec^{-1}, even if the dynamic model is still applicable. This is lower than the rate constant found for cesium systems assuming the dynamic model. Therefore, cation jumping may not show any M_z-dependent line-width phenomena in sodium xanthone and fluorenone, even if the dynamic process is taking place. We are unable to determine the mechanism for sodium systems.

The data shown in Figure 4 give the following thermodynamic quantities for the structure changes of the ion pair, A → B, in cesium xanthone: ΔH = 1.6 and 1.3 kcal in DME and THF, respectively, and ΔS = 6.7 and 5.6 cal deg^{-1} in DME and THE, respectively. Since the simple two-jump model with constant a_A and a_B is not strictly applicable, accurate estimates of the thermodynamic quantities cannot be made for sodium systems. However, the dotted line shown in Figure 1 gives estimates of ΔH = 2.6 kcal and ΔS = 8 cal deg^{-1} for sodium xanthone, assuming that the two-jump dyanmic model is applicable. These values are much smaller than those found for the change from contact to solvent-separated ion pairs.[3b,c] This suggests that the solvation changes associated with ion pair structure changes in ketyls only require slight reorganization of solvation structures. This is in contrast with the dynamic ion pair equilibrium process found in systems such as sodium naphthalene in THF, which requires an actual removal and reinsertion of a solvent molecule to the first solvation sphere. The rate constant determined for the ion pair equilibrium is of the order of 10^8 sec^{-1}.[3b,c] Therefore, it is perhaps not unreasonable that the rate constant for the cation jumping process suggested here is of the order of 10^{10} sec^{-1}. Measurements of the temperature dependence of the line broadening can only be made over relatively small temperature ranges, and no accurate measurements of activation energy are possible, but we estimate E_a for the k_1 process to be 2.8 ± 0.7 kcal.

Effect of the Addition of Small Amounts of Polar Solvents. The effect of the addition of polar solvent

Table I. Thermodynamic Data

System	Solvent	ΔH, kcal	ΔS, cal deg^{-1}		
(A) Structural Changes in Ketyl Ion Pairs					
Xanthone, Na	THF	2.6 ± 0.2	8.0 ± 0.5		
Xanthone, Cs	THF	1.3 ± 0.1	5.6 ± 0.5		
Xanthone, Cs	DME	1.6 ± 0.1	6.7 ± 0.5		
(B) Solvent Exchange between DMF and Ethereal Solvents					
				Temp, °K	K
Fluorenone, Li	MTHF	−0.6 ± 0.2	+9.0	298	250 ± 30
Fluorenone, Li	THF			298	100 ± 10
Fluorenone, Li	DME			298	90 ± 10
Fluorenone, Na	THF	+0.4 ± 0.1	+9.9	298	55 ± 5
Fluorenone, Na	DME	−2.7 ± 0.4	−3.2	298	20 ± 2
Xanthone, Na	DME	−0.6 ± 0.2	+3.2	213	25 ± 2

such as DMSO on the structures of ion pairs has previously been studied by Hogen-Esch and Smid[3a] and Lin and Gendell.[9] Hogen-Esch and Smid noted that very small quantities of DMSO converted a contact ion pair into a solvent-separated ion pair in alkali metal fluorenyl, whereas Lin and Gendell concluded that the addition of DMSO had no effect on the structures of ion pairs of nitrobenzene.

In the ketyl systems studied here, DMF actually replaces THF or DME in the solvent shell of cations and preferably solvates toward cations. This is clearly indicated by the change in magnitude of the alkali metal splittings as DMF is added to the solution. Figure 6 shows such changes of alkali metal splittings for lithium, sodium, and cesium fluorenone and xanthone. The alkali metal splittings approach saturation values at about 10% DMF, and this is understood by assuming that one DMF molecule replaces one ethereal solvent molecule in the first solvation sphere of the cation. If the solvent exchange is 1:1, the exchange process is written as

$$\underset{\text{I}}{R^-M^+(\text{ether})_n} + \text{DMF} \underset{k'}{\overset{k}{\rightleftharpoons}} \underset{\text{II}}{R^-M^+(\text{ether})_{n-1}(\text{DMF})} + \text{ether}$$

$$K = \frac{[R^-M^+(\text{ether})_{n-1}(\text{DMF})][\text{ether}]}{[R^-M^+(\text{ether})_n][\text{DMF}]} \qquad (5)$$

Since epr spectra are taken in the limit of rapid exchange of solvent, the observed metal splitting is the weighted average of forms I and II.

$$a = P_I a_I + P_{II} a_{II} \qquad (6)$$

The ratio of forms I and II is given by

$$R = \frac{P_{II}}{P_I} = \frac{a - a_I}{a_{II} - a} = K\frac{[\text{DMF}]}{[\text{ether}]} \qquad (7)$$

Therefore, plots of R *vs.* [DMF]/[ether] should give straight lines if eq 5 is appropriate for describing the exchange process. Such plots are made for a number of systems, and are given in Figure 7. As shown in Figure 7, the plots give fairly good straight lines for a number of systems when the DMF fraction is less than 10%. If two or more solvent molecules are involved in the exchange process, no straight lines would be obtained for the plot of R *vs.* [DMF]/[ether]. If further replacement of solvent molecules is taking place at higher concentrations, the points are expected to deviate from a straight line. This seems to be the case at higher concentrations of DMF. The values of K estimated for various systems from such plots are tabulated in Table I. It is quite clear that DMF preferably solvates toward positive ions. In general, the equilibrium constants follow the following trends.

$$K(\text{Li}) > K(\text{Na})$$

$$K(\text{MTHF}) > K(\text{THF}) > K(\text{DME})$$

The temperature dependence of the equilibrium constant K is given for several systems in Figure 8. ΔH and ΔS are estimated for a few systems. They are

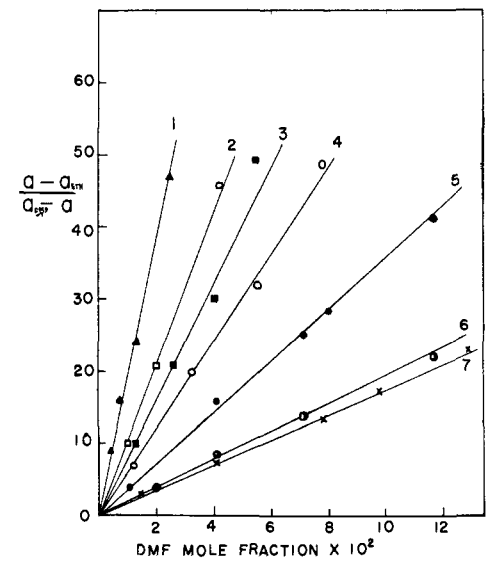

Figure 7. Plot of $(a - a_{\text{ether}})/(a_{\text{DMF}} - a)$ *vs.* mole fraction of DMF: (1) lithium fluorenone, MTHF, 23°; (2) lithium fluorenone, THF, 23°; (3) lithium fluorenone, DME, 23°; (4) sodium fluorenone, THF, 23°; (5) sodium fluorenone, THF, −50°; (6) sodium fluorenone, DME, 23°; (7) sodium xanthone, DME, −58°.

given in Table I. It is seen that ΔH values are generally small, although the signs depend on the system. The interaction between DMF and cation is perhaps stronger than those between ethereal solvents and cations, and therefore the system should gain solvation energy by the solvation with DMF. This reduces the interaction between positive and negative ions as well as the interaction of other solvent molecules with cations. The net effect on ΔH seems to be rather small in all cases studied here. However, realtively large positive entropy changes were observed for THF and MTHF

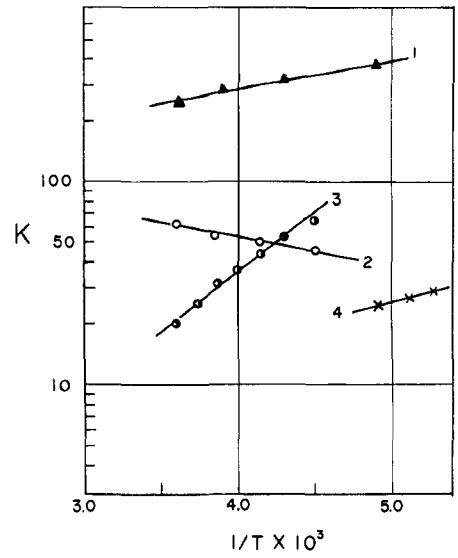

Figure 8. Plot of log K *vs.* $1/T$; solvent exchange between DME and DMF: (1) lithium fluorenone, MTHF; (2) sodium fluorenone, THF; (3) sodium fluorenone, DME; (4) sodium xanthone, DME.

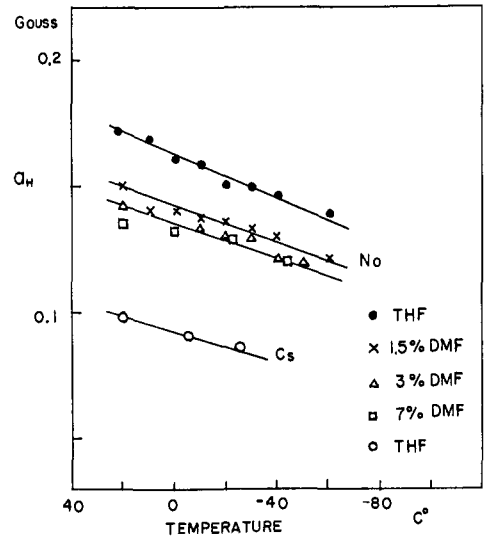

Figure 9. Change of proton splittings by the addition of DMF (protons at 2 and 7 positions, fluorenone): (1) Na, THF; (2) Na, THF + 1.5% DMF; (3) Na, THF + 3% DMF; (4) Na, THF + 7% DMF; (5) Cs, THF.

solvents, indicating a large increase in the freedom of ethereal solvents after solvation by DMF. When DMF solvates the cation, solvation by THF and MTHF seem to decrease more than expected from 1:1 replacement of solvent molecules. On the other hand, ΔS for the DME solution was found to be relatively small. In this case, the solvent-exchange process may be approximately accounted for by a 1:1 exchange process. The different behavior of THF and DME may be expected because of the stronger solvating power of DME. It is also interesting to note that the changes in the alkali metal splittings by replacement of DMF is in the following order: MTHF > THF > DME (Figure 5). The increase in alkali metal splittings was attributed to the change of the average position of the cation more to an off-nodal-plane position with less solvation. When DMF solvates, the cation moves more to an off-nodal-plane position and at the

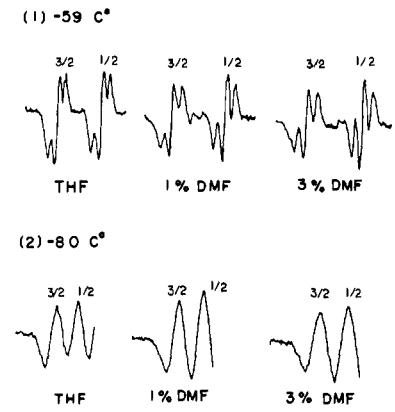

Figure 10. Solvent-exchange-induced M_z-dependent line broadening. The first two peaks of the epr spectra of sodium xanthone: (1) at 59°, (A) pure THF, (B) 1% DMF, (C) 3% DMF; (2) at −80°, (A) pure THF, (B) 1% DMF, (C) 3% DMF Higher modulation amplitudes were used.

same time loses solvation by ethereal solvents. The observed trend in the increase of metal splitting by DMF addition follows the trend of solvation power of solvent. This also indicates the greater loss of solvation by ethereal solvents in the case of weaker solvating solvents after the DMF addition.

Proton Splitting. Although we have not studied in detail the effect of the addition of DMF on proton splittings, the smallest proton splittings ($a_{2,7}$) appreciably decreases after the addition of DMF. The data are shown in Figure 9. This indicates that the electrostatic interaction between cation and anion decreases with the addition of DMF.[7] The solvation of polar DMF molecules reduces the electrostatic interaction between positive and negative charges considerably.

Kinetics of the Solvation Process. Since the sodium splittings change considerably with the addition of DMF, the formation of DMF-solvated ketyls modulates the isotropic hyperfine splittings and thus contributes to the line width. Since the lines corresponding $M_z = \pm {}^3/_2$ for sodium nuclei are more modulated than those for $M_z = \pm 1/2$, M_z-dependent line broadening may be observable if the amplitude of modulation is relatively large and the rate of the solvation process is sufficiently slow. A formula relating the rate of solvent exchange to the M_z-dependent line width can be obtained easily by using the standard line-width formula[20] using the two-jump models. The rate of formation of a DMF-solvated complex is given by

$$k = (2.03 \times 10^7) \frac{P_I^2 P_{II}^2 \left(1 + K \frac{[\text{DMF}]}{[\text{ether}]}\right)}{[\text{DMF}]} \frac{2(a_I^2 - a_{II}^2)}{\Delta H_{\pm 1/2} - \Delta H_{\pm 1/2}} \quad (8)$$

where ΔH_{M_z} are the line widths of the lines corresponding to sodium quantum number M_z. Here we assumed that broadenings due to other causes, such as incomplete rotational averaging of anisotropic hy-

(20) For example, (a) J. Pople, W. G. Schneider, and R. Bernstein, "High-Resolution Nuclear Magnetic Resonance," McGraw-Hill, New York, N. Y., 1969; (b) A. Carrington and A. McLachlan, "Introduction to Magnetic Resonance," Harper and Row, New York, N. Y., 1967, Chapter 12.

Table II. Kinetic Data[a]

System	Solvent	k_1	k_{-1}	E_{a1}	E_{a-1}	A_1	A_{-1}
			(A) Structural Changes in Ion Pairs				
Xanthone, Cs	DME	2.0×10^{10} (−30°)	2.0×10^{10} (−30°)	2.8 ± 0.8	1.2 ± 0.5	7×10^{12}	2×10^{11}
Xanthone, Cs	THF	1.5×10^{10} (−50°)	1.7×10^{10} (−50°)	2.8 ± 0.8	1.4 ± 0.5	8×10^{12}	4×10^{11}
			(B) Solvent-Exchange Process				
		k	k'	E_I	E_{II}	A_I	A_{II}
Xanthone, Na	DME-DMF	1.0×10^8 (−50°)	5×10^6 (−50°)	2.8 ± 0.5	3.4 ± 0.5	$\sim 5 \times 10^{10}$	$\sim 1 \times 10^{10}$
			(C) Association Process				
System		Solvent	k_a		E_a		
Fluorenone, Na		DME-DMF 1:1	1.3×10^9		3.0 ± 0.5		

[a] k_1, k_{-1}, and k', sec^{-1}; k and k_a, M^{-1} sec^{-1}; E, kcal; A, sec^{-1}.

perfine splittings and g factors, are small. Examples of broadening due to solvent-exchange processes are shown in Figure 10. Although the extent of solvation-induced M_z-dependent line broadening is not very large, M_z-dependent line broadening is clearly observable after the addition of a small amount of DMF. If the solvation process is responsible for broadening and eq 8 is applicable, $\Delta H_{\pm 3/2} - \Delta H_{\pm 1/2}$ is proportional to $P_I^2 P_{II}^2[(1/[\text{DME}]) + (k/[\text{DMF}])]$. The plot of $\Delta H_{\pm 3/2} - \Delta H_{\pm 1/2}$ *vs.* $P_I^2 P_{II}^2[(1/[\text{DME}]) + (k/[\text{DMF}])]$ is given for sodium xanthone in Figure 11.

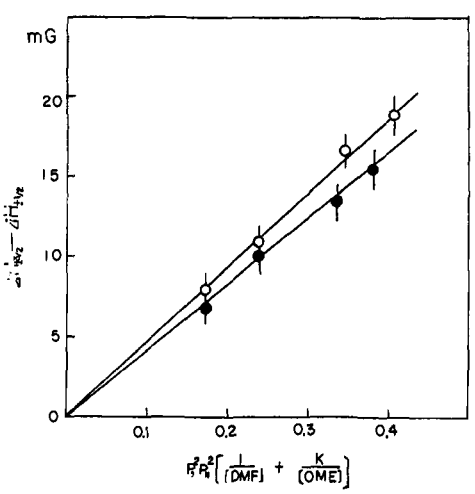

Figure 11 Plot of $\Delta H_{+3/2} - \Delta H_{+1/2}$ *vs.* $P_I^2 P_{II}^2(1/[\text{DMF}] + K/[\text{DME}])$; sodium xanthone in DME-DMF: ○, −80°; ●, −87°.

It is seen that the plots give reasonably good straight lines, and we think this is strong evidence for solvation-induced M_z-dependent broadening.

The rate constants k and k' are estimated from the broadenings. The broadenings of the lines were estimated from the relative intensities of the peaks. Because of incomplete separation of the hyperfine lines, estimates of broadenings have relatively large uncertainties. The plots of k and $\tau = k/k'$ (the lifetime of the DMF-solvated complex) *vs.* $1/T$ are shown in Figure 12. The activation energy for the k process is estimated to be 2.8 ± 0.5 kcal. Extrapolation of low-temperature values to room temperature gives an estimate of k as $\sim 7 \times 10^8$ M^{-1} sec^{-1}. This value is perhaps slightly smaller than a diffusion-controlled rate constant. Kinetic data for solvent-exchange process are given in Table II.

It should be noted here that in each ion pair involved in the solvent exchange process, the cation may be moving rapidly. This motion process within each solvation structure was assumed to be much faster than the solvent-exchange process, as was indicated in the discussion in the previous section. The lifetime of solvated complex is in fact relatively long ($\sim 10^{-7}$ sec^{-1}).

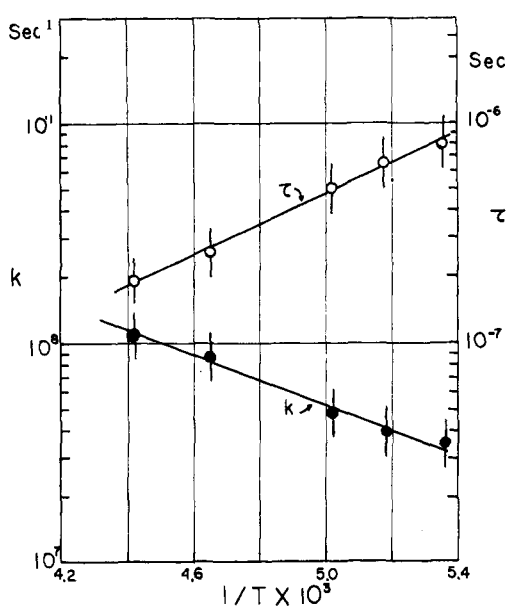

Figure 12. Solvent-exchange rates and lifetimes of DMF complexes; plot of log k and τ *vs.* $1/T$: ○, τ; ●, k. Sodium xanthone in a DME-DMF mixture.

The above example and the other reported in a preliminary note[18] show that epr can be used for studies of the dynamics of solvent-exchange processes.

The Effect of the Addition of Large Amounts of Polar Molecules. (A) Dissociation-Association Equilibria. When the fraction of DMF increases, more than one ethereal solvent is expected to be replaced by DMF molecules. Then the plot of R *vs.* [DMF]/[ether] starts to deviate from a straight line. With more DMF molecules solvating the cation, the electrostatic interaction between positive and negative ions decreases and more dissociation into free ions is expected. In fact, in the case of $\sim 10^{-4}$ M sodium fluorenone in DME solution with 20 vol % DMF, superposition of two epr spectra,

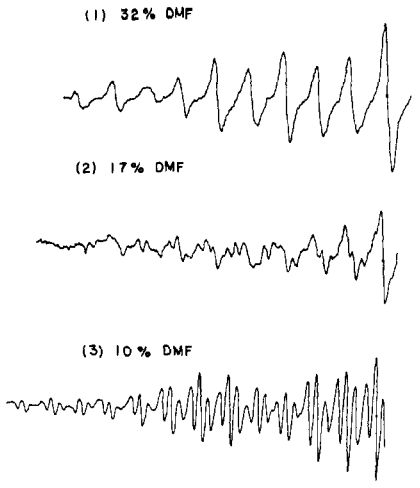

Figure 13. Epr spectra of sodium fluorenone in a mixture of DME and DMF: (1) 32% DMF, (2) 17% DMF, (3) 10% DMF.

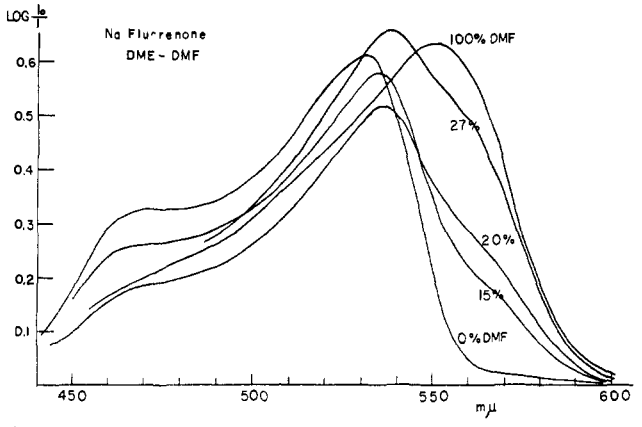

Figure 14. Visible absorption spectra of sodium fluorenone in various mixtures of DMF and DME, concentration $\sim 10^{-4}$ *M*.

one from the ion pair and the other from dissociated ions, was observed. With larger fractions of DMF, the ion pair spectrum completely disappears. An example of the superimposed spectra is shown in Figure 13. The concentration dependence studies clearly show that this is due to an equilibrium between ion pairs and free ions. Thus, the only species which exist in mixtures of DME and DMF are contact ion pairs and free ions, and no solvent-separated ion pairs, such as those found in most hydrocarbon anion systems, were detected over the entire mixing range.[21]

This observation is quite different from the observation of Hogen-Esch and Smid that the fluorenide ion pairs are converted into solvent-separated ion pairs by the addition of very small amounts of a polar solvent such as DMSO. This difference is probably due to the fact that the negative charge is more localized on the carbonyl oxygen and strong ion–ion interaction always dominates the ion solvent interaction. In solutions with large DMF fractions, the ion pair dissociates into free ions, because the dielectric constant of the solvent becomes large and ΔG for dissociation becomes smaller.

The existence of solvent-separated ion pairs depends on the delicate balance between ion–ion interactions and ion–solvent interactions. Favorable conditions for the formation of solvent-separated ion pairs would be:

(21) Alkali metal nmr studies show that the ion pair of ketyls in high concentrations of DMF is a contact ion pair: T. Takeshita and N. Hirota, unpublished observation.

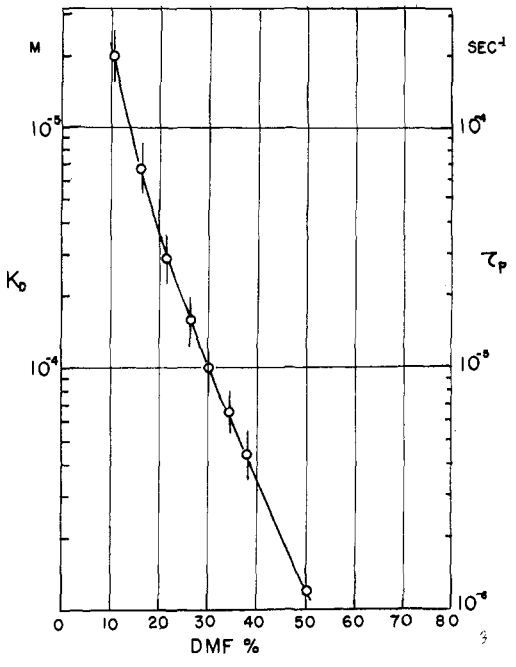

Figure 15. Estimated dissociation constants of sodium fluorenone as functions of DMF fractions. τ_p indicates the estimated lifetimes of ion pairs in different mixtures.

(1) delocalized charge density distribution on the anion, (2) strong solvation of the cation, (3) relatively small dielectric constant of the solvent. Therefore, the structures of the ion pairs strongly depend on the nature of cation, anion, and solvent. One should be very careful in applying conclusions obtained in one system to other systems.

Since the visible absorption of ion pairs and free ions is significantly different, it is possible to make an approximate determination of the dissociation constant of fluorenone ketyls (Figure 14). Log K_D *vs.* the estimated solvent mixing ratio is shown in Figure 15.

(B) Kinetics of Dissociation–Association Equilibria. Although the existence of dissociation–association equilibria has been established in a number of cases from epr studies,[3b,c,13] there seem to be no detailed kinetic studies of such processes.

The process taking place in solutions which contain large fractions of DMF is given as

$$R^-M^+ \underset{k_a}{\overset{k_d}{\rightleftharpoons}} R^- + M^+ \qquad (9)$$

Since the positions of the hyperfine lines of R^-M^+ and R^- are different, careful measurements of line widths should be able to provide the rates of the dissociation and association processes. The spectrum of sodium fluorenone in a solution whose DMF volume fraction is less than 15% primarily consists of the spectrum of ion pair. In the range of 15–20% DMF, one can see the superposition of two spectra.

An analysis of the line width can be obtained by solving the steady-state-modified Block equation[20]

$$\left(\alpha_p + \frac{1}{\tau_p}\right)G_{p_i} = i\gamma H_1 M_{p_i} + \frac{G_f}{4\tau_f} \qquad (10)$$

$$\left(\alpha_f + \frac{1}{\tau_f}\right)G_f = i\gamma H_1 M_f + \sum_i \frac{G_{p_i}}{\tau_p}$$

where p and F indicate ion pair and free ions; i refers to the line corresponding to the ith nuclear spin state of sodium nuclei; notations for G, M, τ, H, and α are those used in standard references.[20] However, the solution of eq 10 for general cases does not give a simple line-width formula, and we only consider the limiting cases here.

In a 17% DMF solution of 5 ± 10^{-5} M fluorenone ketyl, the spectrum is the superposition of those of the ion pair and the free ion. The line widths of ion pair and free ion spectra in this mixture are slightly broader than those in pure DME. The broadening probably does not exceed 20 mG. Using the slow limit solution for eq 10, we can make order of magnitude estimates of τ_p.

$$k_d = \frac{1}{\tau_p} = (1.52 \times 10^7)[\delta H]_p \text{ sec}^{-1} \qquad (11a)$$

$$k_a = \frac{1}{\tau_P[M^+]} = \frac{(1.52 \times 10^7)[\delta H]_f}{[M^+]} M^{-1} \text{ sec}^{-1} \qquad (11b)$$

Here $[\delta H]$ is the broadening due to the kinetic process measured from the point of maximum slope in the derivative curves; values are in gauss. From the limit of $[\delta H]$, we can obtain an estimate of the upper limit of k_a and k_d. From $[\delta H]_p \lesssim 2 \times 10^{-2}$ G, we obtain $k_d \lesssim 3 \times 10^5$. From $[\delta H]_f \lesssim 2 \times 10^{-2}$ G and $[M^+] \cong 2.5 \times 10^{-5}$ M, we obtain $k_a \lesssim 1 \times 10^{10}$ M^{-1} sec^{-1}. The upper limit of k_a is about of the order of a diffusion-controlled rate constant.

In order to obtain better estimates of k_a, k_d, and activation energies for the dissociation–association processes, we have studied the effect of the addition of Na^+ on the line width using 50:50 mixture of DMF and DME. As the source of Na^+ ion, we used Na^+-BPh_4^-. $Na^+BPh_4^-$ is considered to be dissociated in 50:50 mixtures of DME and DMF (Figure 16). The lines become very broad after the addition of 1.7×10^{-3} M Na^+, as shown in Figure 16, but no spectrum of the ion pair is observable. However, the optical spectrum indicates that $[R^-]/(R^-M^+) \sim 1/2$. We think

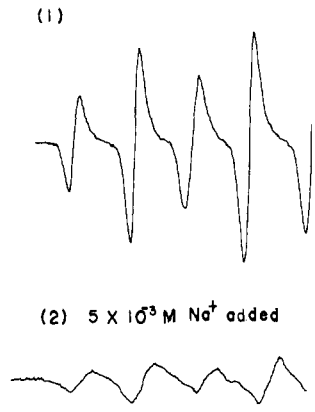

Figure 16. Epr spectra of sodium fluorenone in 50% DMF solution (24°): (A) before the addition of Na^+ ions, (B) after the addition of 5×10^{-3} M Na^+ ion.

that the broadening is due to the dissociation–association process. First we assume that the observed line broadening primarily comes from the broadened free ion peak. Taking $[\delta H]_f = 1.4 \times 10^{-1}$ G and $[M^+] = 1.7 \times 10^{-3}$ M and using eq 10, we obtain $k_a = 1.3 \times 10^9$ M^{-1} sec^{-1} at 25°. This rate constant is considered to be the diffusion-controlled rate constant. We conclude that the rate constant for the association process is close to a diffusion-controlled rate constant. Using $K \sim 10^{-3}$, $k_d = 1/\tau \sim 1.3 \times 10^6$ M^{-1} sec. If the rate constant for the association of ions is 10^9 M^{-1} sec^{-1} and does not change much with the mixing ratio of DMF and DME, one can estimate the lifetimes of ion pairs in solutions of different DMF fractions. This is given in Figure 15. Using $k_3 \sim 10^9$ M^{-1} sec^{-1} and $K = 5 \times 10^{-5}$ M for 17% DMF solution, we obtain $\tau_p = 5 \times 10^{-4}$ sec. This is consistent with the previously estimated limit, $\tau_p \gtrsim 3 \times 10^{-6}$ sec.

Temperature dependence of $[\delta H]_f$ gives an estimate of the activation energy of association processes. This was found to be about 3 kcal mol^{-1}, which is reasonable for the diffusion-controlled reaction.